Proceedings of the Institute of Acoustics

MEASUREMENT OF MUSICAL WIND INSTRUMENTS USING ACOUSTIC PULSE REFLECTOMETRY

D Sharp The Open University, Dept. of Env. and Mech. Eng., Milton Keynes, U.K.
J Buick University of Edinburgh, Dept. of Physics and Astronomy, Edinburgh, U.K.

1. INTRODUCTION

In the acoustical study of musical wind instruments, two types of measurement have proved particularly valuable. One is the measurement of the bore profile; the other is the evaluation of the input impedance, defined as the ratio of the acoustic pressure to the air volume flow rate at the entrance to the instrument. These two quantities are closely related and, in principle, one can be calculated from the other. In practice, however, complications from features such as sideholes limit the accuracy with which the impedance can be calculated from the bore profile.

The most common way of measuring the bore profile of an instrument has been to use tools such as calipers. However, although these direct measurements are very accurate, in many cases it is not possible to access the whole length of the instrument leaving the measured profile incomplete. The input impedance of the instrument has conventionally been measured in the frequency domain. To make the measurement, it is first necessary to measure the volume flow rate. The pressure is then measured at the entrance to the instrument and divided by the volume flow rate to give the input impedance [1, 2, 3]. The method yields good results but is very time-consuming, requiring the initial volume flow rate measurement and then a pressure measurement at each frequency of interest.

Recently, the time domain technique of acoustic pulse reflectometry has begun to be applied to wind instruments [4, 5, 6, 7]. A pulse of sound is injected into the instrument via a source tube and the resulting reflections are analysed to give the input impulse response, from which both the cross-sectional area as a function of axial distance and the input impedance can be calculated. The advantages of acoustic pulse reflectometry are that it only requires a pressure measurement (removing the need for a volume flow rate calibration measurement) and that it is non-invasive (allowing inaccessible bore sections to be measured). As a pulse technique, all frequencies are dealt with simultaneously making acoustic pulse reflectometry less time-consuming than the frequency domain method.

2. DETERMINATION OF INPUT IMPULSE RESPONSE

2.1 Experimental procedure

Figure 1 shows a schematic diagram of the pulse reflectometer used in the present study. The reflectometer and instrument under test are mounted in an anechoic chamber, with the electronics in an adjoining control room.

An electrical pulse is produced by a D/A converter (located on a data acquisition board inside a PC), amplified and used to drive a loudspeaker. The resultant sound pressure pulse travels along a 10.5m long copper source tube of internal radius 4.8mm and wall thickness 1.2mm. A microphone embedded part of the way along the tube records the reflections returning from the instrument under test, which is coupled to the far end of the source tube. The microphone output is amplified and low-pass filtered to prevent aliasing. The resultant signal is then sampled using an A/D converter and stored on the PC.

This procedure is repeated 1000 times and the samples are averaged to improve the signal-to-noise ratio. A short delay is included before each repetition to ensure all the signal from the previous step has died away.

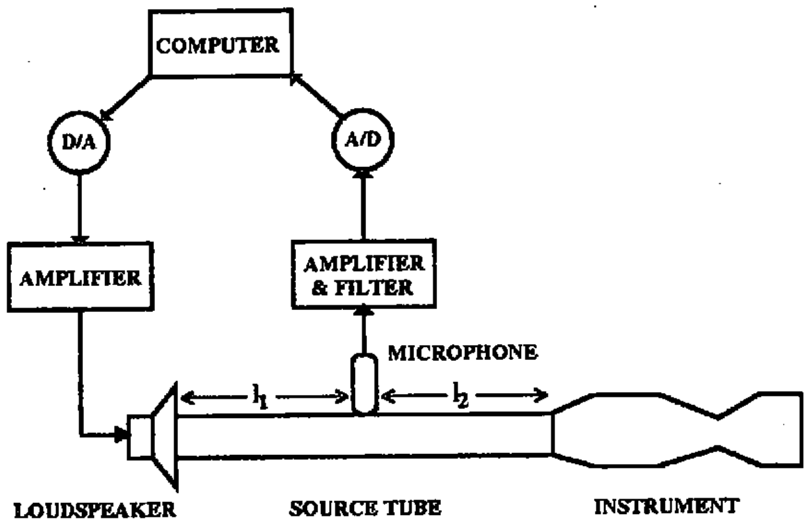

Figure 1 : Schematic diagram of acoustic pulse reflectometer

2.2 Physical constraints on the source tube

The source tube section l_2=3.1m is necessary to ensure that the input pulse has fully passed the microphone before the first of the returning instrument reflections reaches it. The minimum duration of the input pulse is in practice limited by the requirement that the pulse carries sufficient energy to ensure a good signal-to-noise ratio in the measured reflections.

After the instrument reflections pass the microphone they are further reflected by the loudspeaker. The source tube section l_1=7.4m is necessary to separate the instrument reflections from these source reflections. It ensures that once the instrument reflections reach the microphone, they can be recorded for up to $2l_1/c$ seconds (the time taken to travel the distance from the microphone to the loudspeaker and back) before the source reflections return and contaminate the signal.

2.3 Deconvolution

For an ideal delta function sound pressure pulse, the reflections measured by the microphone would be the input impulse response of the instrument under test (or to be more precise, the input impulse response of the source tube section l_2 and the instrument). However, the sound pressure pulse is not ideal; to obtain the input impulse response, the reflections are deconvolved with the input pulse shape. The input pulse shape is measured by terminating the source tube with a perspex cap of thickness 5mm and recording the reflected pulse [8]. This ensures that both the instrument reflections and the input pulse have travelled the same path in the source tube and have therefore experienced the same source tube losses. It also ensures that deconvolution yields the input impulse response of the instrument alone, without a section of source tube included.

The deconvolution is carried out by Fourier transforming both the sample containing the instrument reflections and the sample containing the input pulse. To prevent leakage in the frequency domain, both samples must be self-windowing; i.e. the signal must have decayed to zero by the end of the sample. A complex division of the instrument reflections by the input pulse is then carried out in the frequency domain. A constraining factor q is added to the denominator to prevent division by zero.

$$IIR(\omega) = \frac{R(\omega)I^*(\omega)}{I(\omega)I^*(\omega)+q}$$

where ω is the angular frequency, $R(\omega)$ is the transformed instrument reflections measured at the microphone, $I(\omega)$ is the transformed input pulse measured at the microphone, $I^*(\omega)$ is the complex conjugate of $I(\omega)$ and $IIR(\omega)$ is the transformed input impulse response.

$IIR(\omega)$ is then inverse Fourier transformed to give the input impulse response iir(t) of the instrument.

3. BORE RECONSTRUCTION

The reflections returning from the instrument occur at changes in impedance, such as expansions or contractions along the instrument's bore. A suitable algorithm (such as the layer-peeling algorithm developed by Amir, Rosenhouse and Shimony [9], which compensates for attenuation due to losses) allows the reflection coefficients arising from these impedance changes to be evaluated from the input impulse response. It is then a small step to calculate the changes in area along the bore. If the instrument is assumed to have cylindrical symmetry, the changes in radius can also be calculated.

However, dc offsets in the input pulse and the instrument reflections generally cause a small dc offset in the input impulse response. This offset manifests itself by causing the reconstruction to expand or contract too rapidly. For accurate reconstruction, the offset must be completely removed before application of the reconstruction algorithm.

The dc offset can be determined directly from the input impulse response by inserting a 403mm long steel cylindrical tube (of wall thickness 1.7mm and internal radius 4.7mm, approximately the same as that of the source tube) between the source tube and the instrument under investigation. Since there should be no signal reflected back from this cylindrical connector, the input impulse response should be zero. The average value of the measured input impulse response (of the connector coupled to the instrument) over this range thus gives the dc offset value.

3.1 Brass instrument reconstructions

In this section, reconstructions of two trumpets are presented. Direct measurements are superimposed on the graphs to provide comparison with the reconstructed profiles.

3.1.1 Amati-Kraslice trumpet

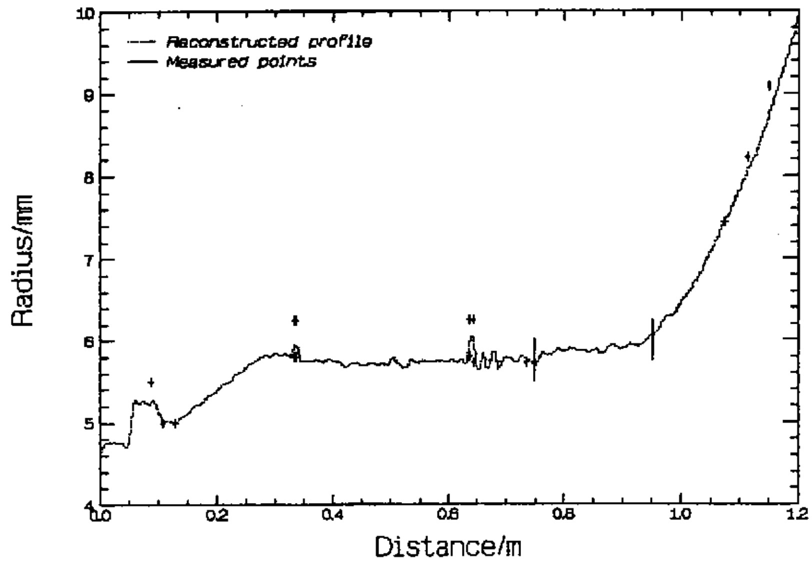

Figure 2 : Reconstructed and measured bore profiles of Amati-Kraslice trumpet. No valves depressed.

Figure 2 shows a bore reconstruction of an Amati-Kraslice trumpet in B♭ with no valves depressed. This instrument is a 'standard model' trumpet.

For the first 100mm, the graph shows the coupler used to connect the instrument to the reflectometer. The coupler penetrated a distance of 13.5mm into the instrument. After 100mm, the graph shows the trumpet profile (starting from a position 13.5mm in from the mouthpiece end).

After an initial widening of the bore, the profile of the trumpet is approximately cylindrical. The radius remains fairly constant through the valve section which is situated towards the end of the instrument. This constant bore radius is characteristic of a 'standard model' trumpet. At the bell, the radius begins to increase rapidly.

Comparison of the reconstructed profile with radii directly measured at various accessible positions along the trumpet bore reveals that the reconstruction breaks down in regions where the bore radius changes rapidly. Prime examples of such regions are the steps at the beginning and end of the main tuning-slide (at 340mm and 630mm respectively on the graph) and the flaring bell. In these regions, the reconstructed profile has a smaller radius than the directly measured radius. The most likely explanation for this breakdown is the fact that the reconstruction algorithm assumes plane wave propagation within the instrument. At regions of rapid change in the bore profile, spherical wave propagation becomes predominant.

3.1.2 Rudall Carte 'Webster' trumpet

Figure 3 shows a bore reconstruction of a Rudall Carte 'Webster' trumpet in B♭ with no valves depressed. This instrument is a 'conical bore model' trumpet.

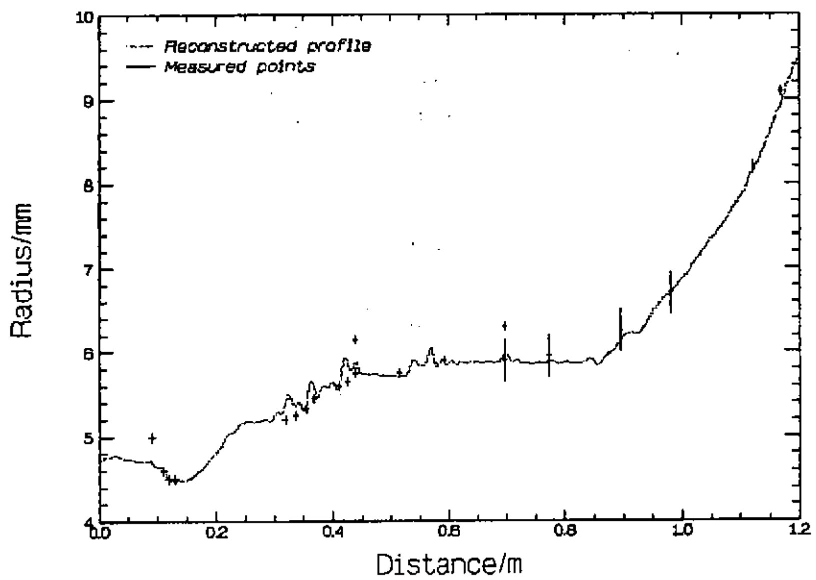

Figure 3 : Reconstructed and measured bore profiles of Rudall Carte 'Webster' trumpet. No valves depressed.

For the first 100mm, the graph shows the coupler used to connect the instrument to the reflectometer. The coupler penetrated a distance of 10.0mm into the instrument. After 100mm, the graph shows the trumpet profile (starting from a position 10.0mm in from the mouthpiece end).

After an initial widening of the bore, the profile of the trumpet continues to expand slowly. The radius increases through the valve section which, unlike the Amati-Kraslice trumpet, is situated towards the start of the instrument. This continual slow expansion of the bore is characteristic of a 'conical bore' trumpet. At the bell, the radius increases more rapidly.

Again, comparison of the reconstructed profile with radii directly measured at various accessible positions along the trumpet bore reveals that the reconstruction breaks down in regions where the bore radius changes rapidly (such as the steps at the ends of tuning-slides and the flaring bell).

4. INPUT IMPEDANCE

The input impulse response is a measure of the amount of input signal reflected at discrete distances along the instrument. As the reflections are caused by changes in impedance within the instrument, it is clear that the input impulse response and the input impedance are closely related. Indeed, the complex input impedance of an instrument may be evaluated from its input impulse response. The analysis assumes plane wave propagation within the source tube.

In the time domain

$$p(t) = \delta(t) + iir(t)$$

$$z_{st} \times u(t) = \delta(t) - iir(t)$$

where p(t) is the pressure recorded by the microphone at time t deconvolved with the input pulse shape, u(t) is the volume velocity at the microphone at time t, $z_{st}=\rho c/S$ is the acoustic impedance of the source tube (ρ is the air density, c is the speed of sound in air, S is the cross-sectional area of the source tube) and iir(t) is the input impulse response of the instrument.

In the frequency domain this gives

$$P(\omega)=1+IIR(\omega)$$

$$z_{st}\times U(\omega)=1-IIR(\omega)$$

where P(ω) is the Fourier transform of p(t), U(ω) is the Fourier transform of u(t) and IIR(ω) is the Fourier transform of iir(t).

Hence, the input impedance is given by:

$$z(\omega)_{in}=\frac{P(\omega)}{U(\omega)}=z_{st}\times\frac{1+IIR(\omega)}{1-IIR(\omega)}$$

4.1 Brass instrument impedance curves

In this section, impedance curves for two cornets measured using acoustic pulse reflectometry are presented. For comparison, impedance curves measured using a conventional frequency domain technique (the swept sine wave technique) are included on the graphs.

In the swept sine wave technique, the instrument under test is excited at its input by a sinusoidal pressure wave supplied via a high impedance capillary. The frequency of the excitation wave is increased and the pressure response at each frequency is recorded. On the assumption that the impedance of the capillary is independent of frequency and much larger than the impedance of the instrument, the excitation wave can be considered to have a constant volume flow rate. The recorded pressure response is then directly proportional to the input impedance of the instrument. Thus, the input impedance is determined by dividing the pressure response by the volume flow rate.

4.1.1 Boosey & Co. cornet

Figure 4 shows impedance curves for a Boosey & Co. 'Acme' model cornet in B♭. The Boosey & Co. cornet is a 'standard model' cornet with a cylindrical bore through the valves. It has had its playing pitch lowered from A_4=452.5 Hz to 440Hz by the insertion of cylindrical extension pieces in its main tuning-slide.

The basic shape of the two curves is the same and the frequencies of the resonances and anti-resonances are in good agreement. However, the impedance peaks are generally higher and the troughs lower for the curve measured using the frequency domain technique. This is particularly apparent at the higher frequencies. The most likely explanation for these differences lies with the frequency domain measurement system. At higher frequencies, the capillary ceases to be frequency independent and resonance effects begin to occur. It is also apparent that the assumption that the impedance of the instrument is negligible when compared with the capillary impedance is not entirely correct. The cornet impedance peaks are of the order of 10^8 ohms which is only ten times smaller than the capillary impedance which is of the order of 10^9 ohms.

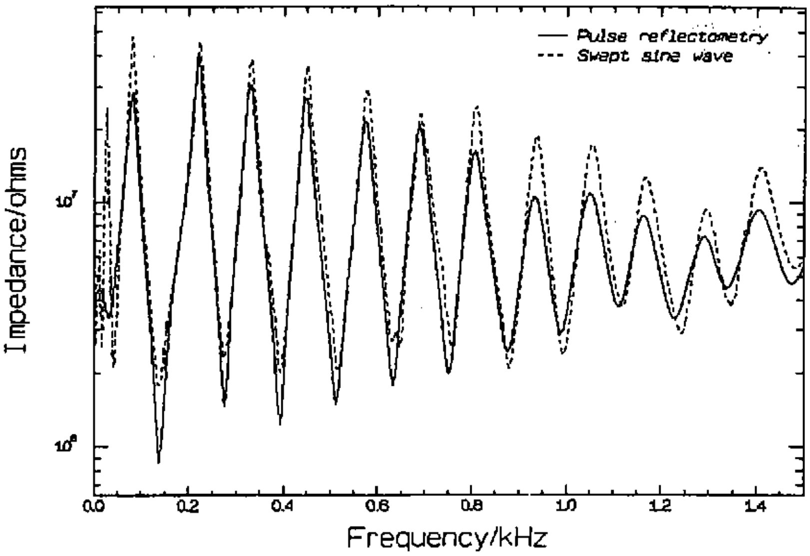

Figure 4 : Impedance curves for Boosey & Co. cornet with no valves depressed.

4.1.2 Rudall Carte cornet

Figure 5 shows impedance curves for a Rudall Carte 'conical bore model' cornet in B♭. The Rudall Carte cornet is characterised by its bore which increases in diameter through the valve pistons and between one valve and the next. Compared with the Boosey & Co. cornet, the bore is narrower and more gently tapering between the mouthpiece receiver and the valves. The instrument was designed to play at a pitch of A_4=452.5Hz.

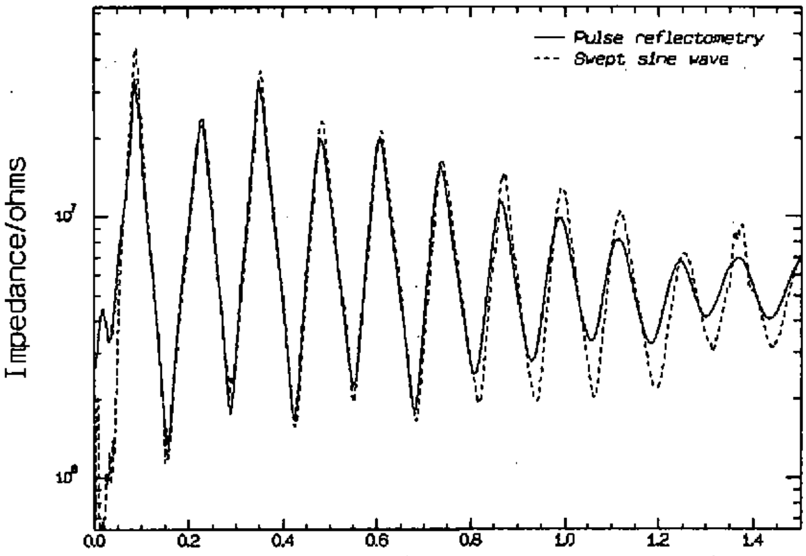

Figure 5 : Impedance curves for Rudall Carte cornet with no valves depressed.

Again, the basic shape of the two curves is same with the frequencies of the resonances and anti-resonances in good agreement. As before, the impedances are higher for the peaks and lower for the troughs for the curve measured using the frequency domain technique.

4.2.3 Discussion

Comparison of the curves for the two cornets clearly shows that all the peaks are at slightly lower frequencies for the Boosey & Co. cornet which has had its pitch lowered. In fact, analysis of the frequencies of the peaks suggest that the Boosey & Co. cornet should play at a pitch around 116 cents lower than the Rudall Carte instrument. Playing tests confirm that this is indeed the case. It appears that the high pitch instrument was designed to play at A_4 with its tuning-slides partially withdrawn.

5. CONCLUSIONS

Acoustic pulse reflectometry has proved itself a useful tool in the study of musical wind instruments. It enables quick and accurate non-invasive measurement of both internal profile and input impedance. Knowledge of these quantities is of vital importance when investigating and comparing the physical characteristics and playing properties of wind instruments.

6. REFERENCES

[1] Backus J (1975). "Input impedance curves for the reed woodwind instruments." J.Acous.Soc.Am., 56(4), 1266-1279.

[2] Pratt RL, Elliott SJ and Bowsher JM (1977). "The measurement of the acoustic impedance of brass instruments." Acustica, 38, 236-246.

[3] Causse R, Kergomard J and Lurton X (1984). "Input impedance of brass musical instruments – Comparison between experiment and numerical models." J.Acous.Soc.Am., 75(1), 241-254.

[4] Smith RA (1988). "It's all in the bore!" Inttemational Trumpet Guild Journal, 12(4).

[5] Watson AP and Bowsher JM (1988). "Impulse measurements on brass musical instruments." Acustica, 66(3), 170-174.

[6] Sharp DB, Myers A, Parks R and Campbell DM (1995). "Bore reconstruction by pulse reflectometry and its potential for the taxonomy of brass instruments." Proc. of the 15th International Congress on Acoustics, Trondheim, Norway; pp.481-484.

[7] Sharp DB, MacGillivray TJ, Ring W, Buick JM and Campbell DM (1998). "Acoustical comparison of bassoon crooks." International Symposium on Musical Acoustics, Seattle; pp. 209-214.

[8] Sondhi MM and Resnick JR (1983). "The inverse problem for the vocal tract: numerical methods, acoustical experiments, and speech synthesis." J.Acous.Soc.Am., 73(3), 985-1002.

[9] Amir N, Rosenhouse G and Shimony U (1995). "A discrete model for tubular acoustic systems with varying cross section – The direct and inverse problems. Parts 1 and 2: Theory and experiment." Acustica, 81(5), 450-474.